
**THE IMPACT
OF HIGH-INTENSITY ULTRASOUND
ON LIQUIDS**

**Droplet Ejection from an Interface between Two Immiscible Liquids
under Pulsed Ultrasound**

A. P. Brysev^{1,2*}, F. Zoueshtiagh^{2}, P. Pernod^{2***},
V. L. Preobrazhensky^{1,2****}, and D. Makalkin^{1,2*****}**

*Joint International Laboratory on Critical and Supercritical Phenomena in Functional Electronics,
Acoustics and Fluidics (LIA LICs):*

¹*Wave Research Center, Prokhorov General Physics Institute, Russian Academy of Sciences,
ul. Vavilova 38, Moscow, 119991 Russia*

²*University of Lille, CNRS, Centrale Lille, UMR 8520, Institute of Electronics, Microelectronics
and Nanotechnology, F-59000 Lille, France*

Received December 24, 2015

Abstract—The emphasis of this study is on the ejection of single droplets of a certain size under pulsed ultrasound. Droplet ejection from an interface of two immiscible liquids in this mode, which differs from the well-known ultrasonic fountain (where liquid droplets arise spontaneously), has been experimentally implemented and investigated. The spatial and time evolution of the interface deformation and violation of interface integrity, caused by pulsed acoustic radiation pressure, has been recorded with a high-speed video camera. It is shown that, depending on the ultrasound intensity, three characteristic modes of interface response can be distinguished. In the first (low-intensity) mode, the interface undergoes forced oscillations, without violation of its integrity. In the second (intermediate-intensity) mode, which is in the focus of our study, the interface integrity is violated due to the ejection of a single droplet of a certain size; the latter continuously changes its shape when moving in the second liquid. In the third (high-intensity) mode, the predictable ejection of droplets of a predictable size turns into stochastic ejection of multiple droplets with unpredictable sizes. The dependence of the sizes of single droplets on the parameters of focused ultrasound beam have been measured in the second (stable) mode of ultrasound ejection. Based on these measurements, the range of ultrasound parameters providing controlled generation of single droplets of a specified size is estimated. Differences in the dynamics of interface motion and specific features of droplet generation for the liquid/liquid interface in comparison with the liquid/gas interface are indicated. Possible applications of the observed effects are discussed.

DOI: 10.3103/S1541308X16030080

1. INTRODUCTION

The study of the transformation of acoustic energy in liquids into other forms of energy began in 1927, when experiments with high-intensity acoustic beams were performed at the Loomis Laboratory in Tuxedo Park, N.Y. These experiments revealed for the first time that an installation of a high-power acoustic source on the bottom of a bath with oil gives rise to a bulge on the oil surface (erupting oil droplets like a miniature volcano) [1]. The improvements made in the 1950s–1960s were aimed at increasing the sound

intensity by localizing acoustic energy in acoustic waveguides or using acoustic lenses. Under these conditions, one could observe continuous droplet ejection in the form of a geyser or formation of structures on the liquid surface, in which some perturbations were sufficiently strong to tear off droplets [2]. In the end of the 1960s, this process was used in commercial inhalers to form drugs in the form of mist [3]. In the beginning of the 1970s, researchers started developing a new approach aimed at forming single droplets by applying less intense (on average) ultrasound; this process was implemented with the aid of pulsed focused acoustic beams (drop-on-demand technique) [4]. The significant progress in the automation and robotization of the drop-on-demand technique, stimulated by the need for exact dosing of liquids (which arose in the 2000s), made

*E-mail: brysev@ya.ru

**E-mail: farzam.zoueshtiagh@univ-lille1.fr

***E-mail: philippe.pernod@ec-lille.fr

****E-mail: preobr@newmail.ru

*****E-mail: dmitrymakalkin@yandex.ru

it possible to adapt the acoustic drop ejection (ADE) technology to small volumes of liquids (several micro- and even pikoliters) [5]. Currently, this technology is well-developed; it is applied in high-quality printers, spectrum analyzers for liquids, modern technologies in biology, chemistry, and food and pharmaceutical industries, and many other engineering applications, where precise control of small liquid volumes is necessary. In addition, since ADE is a contactless technology, it allows one to perform remotely necessary manipulations, for example, when carrying out on-Earth-controlled manipulations with liquids on orbit or in the far space. It may be irreplaceable in some cases, for example, when dealing with toxic or radioactive liquids. Finally, the study of the ultrasonic pipette physics is urgent in view of the intense development of new-generation functional microstructures with tunable morphology (“lab-on-chip” structures) [6, 7].

At the same time, it should be noted that all above-said holds true for the ultrasound impact on the liquid/gas interface, whereas the progress in the study with the liquid/liquid interface is much less significant. Concerning the latter case, we should note studies [8, 9], where the deformations of a sound-transparent water–chloroform interface located in the focal plane of intense ultrasound beam were investigated to verify the Langevin theory of acoustic radiation pressure. It was shown that, in the case of low-amplitude deformations, the experimental results obtained for both stationary and dynamic modes of ultrasound impact on the interface are in good agreement with the theoretical predictions. For higher amplitude deformations, the interface takes a peculiar (keyhole) shape. It was found that the interface behavior depends on the direction of focused ultrasound beam and that the interface dynamics is qualitatively similar to that observed under laser excitation [10, 11]. Finally, at even higher sound intensities, effects of ultrasonic fountain or jet were observed in the focal region.

In this study, we experimentally implemented and analyzed three characteristic modes, which replace one another with an increase in the intensity of ultrasound impact on an interface between two immiscible liquids:

- (i) forced interface oscillations, which do not lead to droplet ejection;
- (ii) ejection of individual droplets, whose size can be controlled in a certain range by changing the ultrasound beam parameters;
- (iii) multiple and random ultrasound droplet ejection.

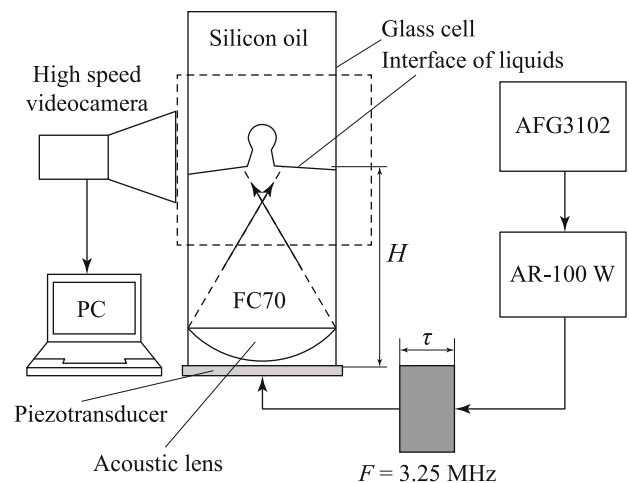


Fig. 1. Schematic of the experimental setup. Dashed lines with arrows indicate the ultrasound beam direction, and the dashed-line rectangle is the video recording area.

2. EXPERIMENTAL

Experiments were performed in a cylindrical acoustic glass cell with the following sizes: height $H = 56$ mm, external diameter 18.8 mm, and internal diameter 16.4 mm (Fig. 1). The cell was filled with two immiscible liquids: perfluorotripropylamine (Fluorinert FC70) (density 1940 kg m^{-3} , sound velocity 687 m s^{-1} , viscosity 12 cS) and silicone oil (density 853 kg m^{-3} , sound velocity 919 m s^{-1} , viscosity 1.5 cS). A focused ultrasound transducer, coaxially mounted on the cell bottom, had a resonant frequency $f_0 = 2.7 \text{ MHz}$, an aperture of 15 mm, and a focal length $F_0 = 17 \text{ mm}$ (in FC70). RF pulses for ultrasound excitation were formed in a Tektronics AFG3102 functional generator and then amplified by

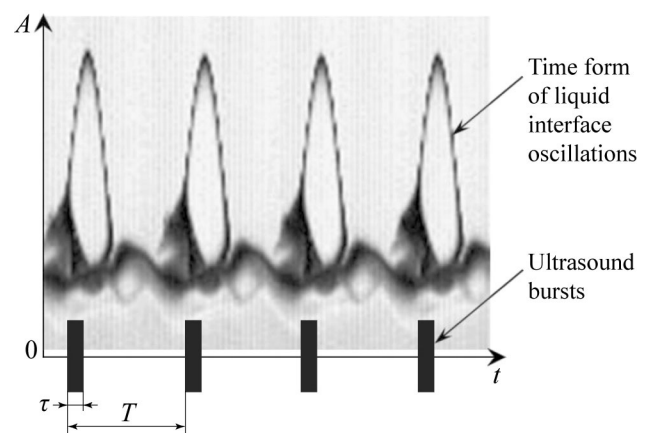


Fig. 2. Typical time form of liquid/liquid interface oscillations, recorded in the middle cross section of the cell and excited by a sequence of ultrasound RF pulses (are schematically shown below, with common time axis t); $T = 500\text{--}1000$ ms.

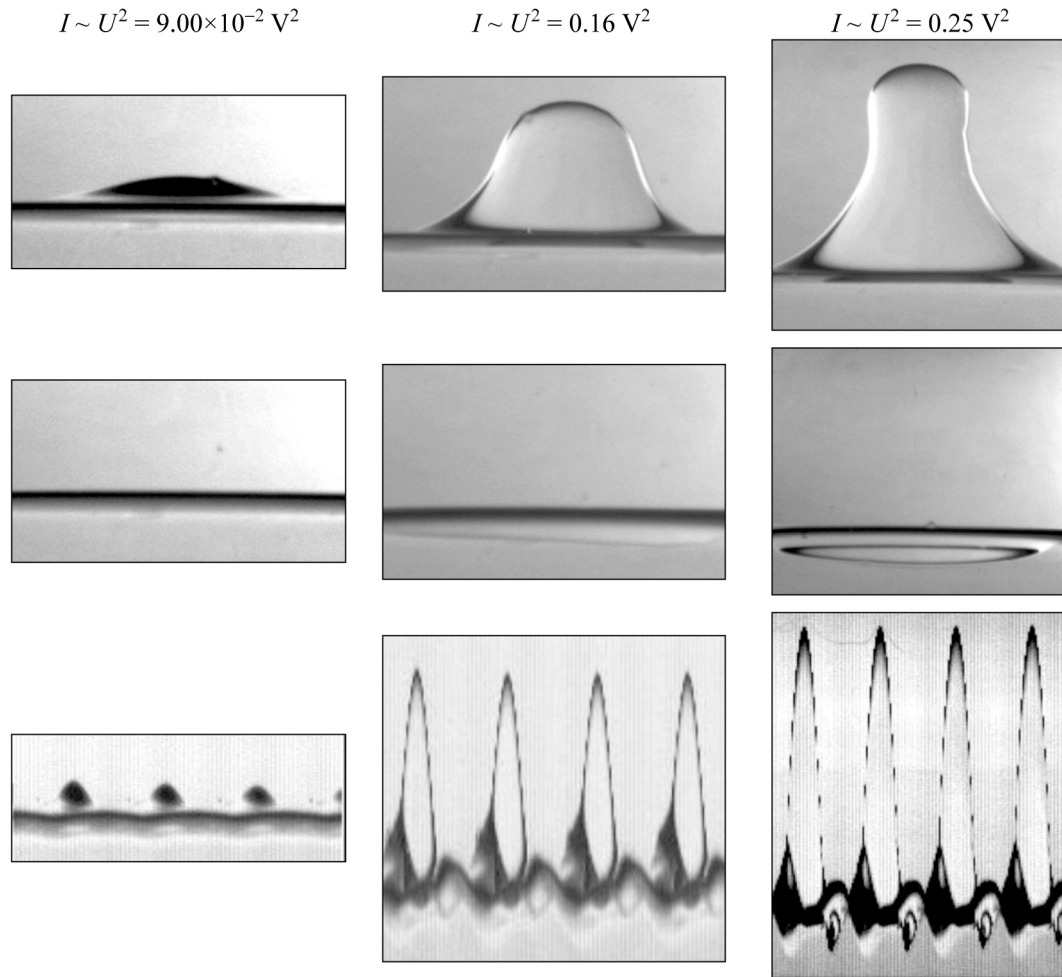


Fig. 3. Spatial distribution of the interface deformation typical of the first mode of pulsed periodic ultrasound impact on interface (the upper and intermediate rows correspond to the maximum upward and downward deflections, respectively) and the corresponding time forms of interface oscillations on the acoustic cell axis (the lower row).

a broadband amplifier with a nominal output power of 100 W. The spatial and time evolution of the interface between the liquids, deformed by pulsed ultrasound radiation pressure, and the formation of droplets were recorded with a speed of 210 frames per second and a resolution of 640×480 pixels, using a high-speed IMPERX IPX-VGA 210 video camera, mounted perpendicular to the common axis of the converter and cell. The recording time, determined by the conditions of specific experiment, was varied from 1.5 to 3.0 s. The recorded digital images were analyzed using the ImageJ software. This software made it possible to determine all necessary parameters of the spatial and time dynamics of the liquid/liquid interface: the amplitude and time form of interface oscillations at any point, the spatial distribution of deformations, and the shape and cross section of single droplets. To exclude the formation of ultrasonic fountain, undesirable in the case under consideration, the maximum duration of ultrasound pulses in all

experiments did not exceed 30 ms. This time is much shorter than the excitation period $T = 500 - 1000$ ms (Fig. 2).

The time form of interface deformation at a certain point was found by synthesizing an image consisting of a sequence of columns, selected from each successive frame of the initial video recording and corresponding to the chosen interface point. Note also that the time of upward interface deflection significantly exceeds ultrasound pulse duration τ .

3. RESULTS AND DISCUSSION

3.1. Mode of Forced Interface Oscillations Not Leading to Droplet Ejection

In accordance with the aforementioned ultrasound intensity levels, one can select three characteristic modes of spatial and time dynamics of liquid/liquid interface deformation. In the first mode, where the ultrasound intensity is below the first threshold value

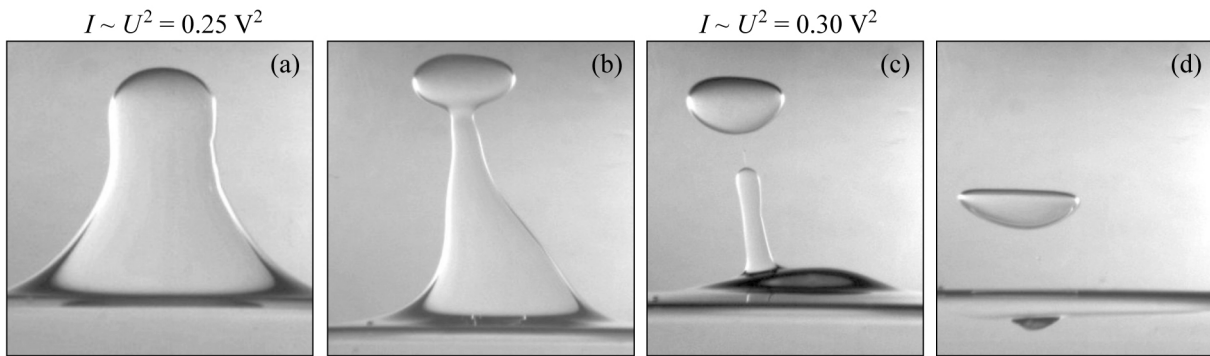


Fig. 4. Different stages of the second mode ($I_{cr1} < I_2 < I_{cr2}$) of pulsed ultrasound impact on interface: (a) formation of a keyhole on the top of the liquid/liquid interface deformed by ultrasound, (b) formation of a droplet, (c) detachment of single droplet from the interface, and (d) the same droplet as in panel (c) before falling on the interface.

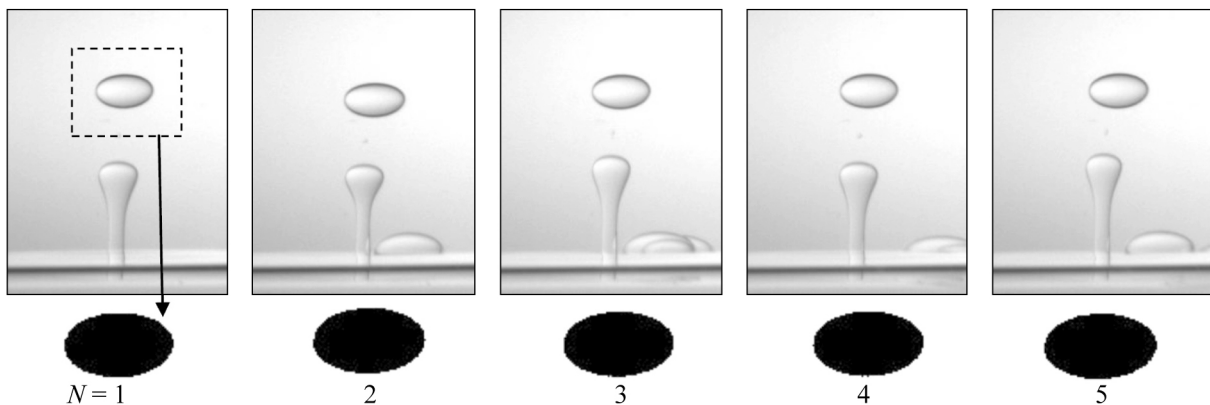


Fig. 5. Successive (from pulse to pulse in one series) photographs of ultrasound ejection of higher density FC70 droplets into lower density silicone oil with a viscosity of 1.5 cS (the first row) and the images of the same droplets transformed into a binary code (N is the number of ultrasound pulses in series). The rectangle in the left image of the upper row and the arrow directed to the second row illustrate the principle of digital image processing and the measurement of droplet cross section. The output voltage of the AFG3102 generator is $U_{pp} = 1.70$ V; the ultrasound pulse duration is $\tau = 1.87$ ms.

I_{cr1} ($0 < I_1 < I_{cr1}$) and is insufficient for tearing off droplets, only forced interface oscillations occur. As can be seen in Fig. 3, the time form of interface oscillations is significantly asymmetric. After reaching the maximum height, the interface moves downwards under the restoring forces of gravity and surface tension. Due to the inertia, the interface passes through the initial horizontal level; however, one can see that the amplitude of its downward deflection is much smaller than the amplitude of upward bending because of the effect of the viscosity and restoring buoyancy and surface tension forces. Note that, for ultrasound of sufficiently high intensity (see the image in the upper row in Fig. 3 at $I \sim U^2 = 0.25$ V²), the shape of the interface deformation looks like a keyhole (a similar observation was reported in [10]). The further increase in the peak-to-peak amplitude of interface deformation with the ultrasound intensity is impeded by the droplet ejection (which is considered in the next section).

3.2. Mode of Ultrasound Ejection and Control of Individual-Droplet Sizes

The second mode is implemented at higher ultrasound beam intensities at the interface ($I_{cr1} < I_2 < I_{cr2}$). In this case, the interface integrity in the upper part of the keyhole is violated due to the formation of a single FC70 droplet (Figs. 4(a,b)), the size of which is reproduced for each subsequent ultrasound pulse. Then the droplet is detached from the interface and moves under the gravity force in silicone oil (Figs. 4(c,d)). In contrast to the well-known effect of ultrasonic fountain, characterized by the random formation of many droplets of different sizes (see, e.g., the image in Fig. 9, obtained at high ultrasound intensities: $I_{cr2} < I \sim U^2$) or even a liquid jet; this feature can be used for *controlled formation of single droplets of a specified size*. Hence, this effect should be investigated more carefully.

Specifically, two basic questions call for accurate quantitative analysis.

(i) What is the error with which the shape and sizes of droplets are reproduced in a periodic sequence of ultrasound pulses in the mode under consideration?

(ii) Can the droplet size be controlled using ultrasound and, if so, in what range?

The answer to the first question is given in Fig. 5, which shows images of droplets obtained in one measurement series, which successively correspond to the ultrasound pulses (N is the number of pulses in series).

The photographs in Fig. 5 were obtained under the following experimental conditions: ultrasound RF pulse repetition period $T = 1000$ ms, pulse carrier frequency $F = 2.7$ MHz, pulse duration $\tau = 1.87$ ms, output voltage of AFG3102 generator $U_{pp} = 1.70$ V, and camera exposure time $55 \mu\text{s}$ (as can be seen in Fig. 5, this time is quite sufficient to form a sharp image of a moving droplet); the liquid/liquid interface was located in the focal plane of piezoelectric transducer, i.e., at a distance of 17 mm from it. To compare most correctly the sizes of droplets, continuously changing their shape when moving in silicone oil, the sequence of images for quantitative analysis of droplet size was selected (using the ImageJ program) from the video recording of a chosen series so as to satisfy the following requirement: time interval T between the images in the sequence must be the same as the ultrasound pulse repetition period. To measure the droplet cross section, a rectangular area containing a droplet image was selected in these photographs (see the left image in the first row in Fig. 5), which was then transformed into a binary code (see the first image in the second row in Fig. 5). This transformation made it possible to separate the droplet image from all foreign elements and calculate automatically (by means of ImageJ program tools) its cross section with a high (\pm few pixels) accuracy, which provides a relative error of this operation less than 1%. The calculation results are presented in Fig. 6.

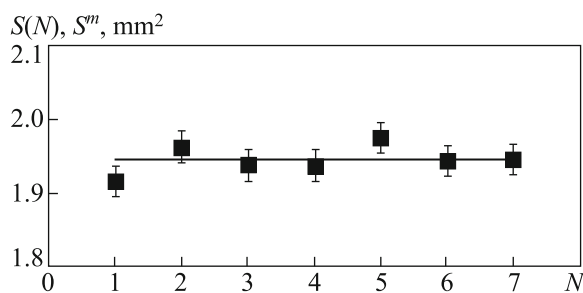


Fig. 6. Dependence of the droplet cross-sectional area S (in the binary code image) on the number of ultrasound pulses N in series. The mean droplet cross section is $S^m = 1.945 \text{ mm}^2$ (horizontal solid line), with a standard deviation $\Delta S = 0.021 \text{ mm}^2$.

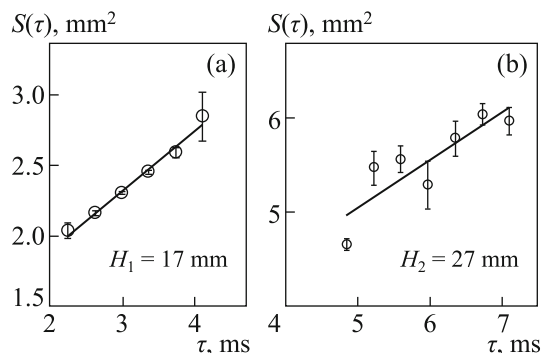


Fig. 7. Dependence of droplet cross section S on ultrasound pulse duration τ (at $I = \text{const}$) for two distances between the liquid/liquid interface and the cell bottom: (a) $H_1 = 17$ mm and (b) $H_2 = 27$ mm for the right plot (the transducer focal length is $F_0 = 17$ mm).

The data in Fig. 6 indicate that the mean droplet cross section in this series is $S^m = 1.945 \text{ mm}^2$, with a standard deviation $\Delta S = 0.021 \text{ mm}^2$. Thus, the accuracy in reproducing the droplet size is not worse than 1.1%. This result, very good from the experimental point of view, is quite sufficient for many applications.

Before presenting the results concerning the second question, we should note that the dynamics of ultrasound droplet ejection from liquid/liquid interface, which is considered here, differs from that for liquid/gas interface. In particular, in the latter case, due to the dominance of surface tension forces, a newly formed droplet always has a spherical shape, which does not change during its motion. The reason is that gas barely affects the shape of droplets at the velocities with which they move after detaching from the liquid surface. In contrast to the gas environment, the liquid significantly affects the droplet shape, which continuously changes during droplet motion in the viscous and dense liquid (see Fig. 4). As a consequence, the cross section of droplet also continuously

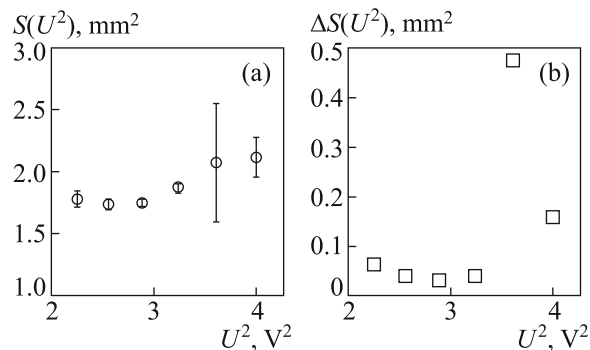


Fig. 8. Dependences of droplet cross section S (a) and standard deviation ΔS (b) on squared output voltage U^2 of the AFG3102 generator (in essence, on ultrasound pulse intensity I) at a constant pulse duration τ .

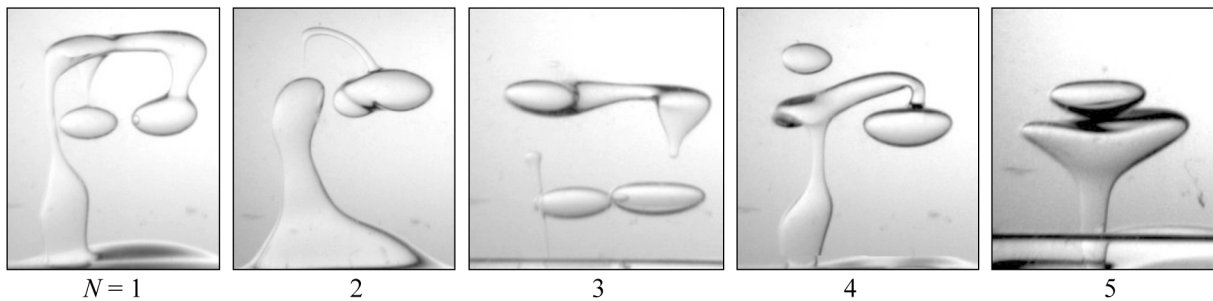


Fig. 9. Photographs illustrating the multiple and random ejection of higher density FC70 droplets into lower density silicone oil with a viscosity of 1.5 cS, which occurs under irradiation of the liquid/liquid interface by a series of successive ultrasound pulses in the third mode (N is the number of pulses in series).

changes during its motion in the upper liquid. At the same time, it is obvious that the volume of the droplet whose velocity in the liquid is not very high remains invariable. With due regard to these considerations, the frame selection rule for subsequent cross-section measurements, which is described in the comments to Fig. 5, was supplemented with another condition. Specifically, the frames from the recorded series in which the droplet shape can be assumed close to ellipsoidal (for example, as in Fig. 5) were chosen. With these two conditions fulfilled, the cross-section measurements (and, when necessary, droplet volume estimations) turn out to be more correct.

The dependence of droplet cross section S on ultrasound pulse duration τ (at $I = \text{const}$) for two distances ($H_1 = 17$ mm, $H_2 = 27$ mm) between the liquid/liquid interface and the cell bottom is shown in Fig. 7. Here, the procedure of calculating area S remained the same as described previously for Figs. 5 and 6.

The plots in Fig. 7 demonstrate a linear (with a rather high accuracy) dependence of droplet cross section S on ultrasound pulse duration τ . The intersection point of the approximating straight line with the time axis yields an estimate for the pulse duration threshold: $\tau_{\text{cr1}} \approx 1$ ms (a) and $\tau_{\text{cr1}} \approx 3$ ms (b); above this threshold, ultrasound droplet ejection starts under these conditions. An estimation of the second critical value of ultrasound pulse duration, above which the third mode (stochastic multiple droplet ejection) begins, yields $\tau_{\text{cr2}} \approx 5$ ms (a) and $\tau_{\text{cr2}} \approx 8$ ms (b). Based on the data in Fig. 7, one can draw another conclusion (important for applications): the range of ultrasonic droplet size control can be varied in certain limits by choosing the corresponding distance between the interface and focal plane.

Figure 8 shows the measured dependences of droplet cross section S (a) and standard deviation ΔS (b) on squared output voltage U^2 of the AFG3102 generator (in essence, on ultrasound pulse intensity I) at a constant pulse duration τ . In contrast

to the plots in Fig. 7, no significant dependence of S on ultrasound intensity I is observed within the measurement error. Only the droplet ejection velocity and, correspondingly, the ejection height increase with ultrasound intensity.

3.3. Mode of Multiple and Random Ultrasound Droplet Ejection

If the ultrasound intensity exceeds the second critical level, the character of droplet ejection sharply changes. Instead of regular ejection of single droplets, one can observe ejection of several droplets with uncontrolled shape and sizes. As an illustration of the processes occurring in the third mode, Fig. 9 shows photographs of several droplets of higher density FC70 liquid in lower density silicone oil, which are formed as a result of irradiation of the liquid/liquid interface by one series of successive ultrasound pulses (N is the number of ultrasound pulses in series). A comparison of the images in Figs. 5 and 7 from the point of view of the difference between the second and third modes is fairly descriptive and illustrative.

4. CONCLUSIONS

In this study, we experimentally implemented and analyzed three characteristic modes of focused ultrasound beam impact on an interface between two immiscible liquids: (i) occurrence of only forced interface oscillations without droplet ejection, (ii) ejection of single droplets of a certain size, and (iii) multiple and random droplet ejection. It was found that, at ultrasound intensities in the range between the first and the second critical values (i.e., in the second mode), the droplet size reproducibility from pulse to pulse is high, and ultrasonic control of droplet size can be implemented. It is shown that the control range can be varied in certain limits by choosing the corresponding distance between the interface and focal plane.

The first mode of ultrasound action can be useful when studying different aspects of the spatial and time dynamics of an interface between liquids enclosed in a small volume and when developing contactless methods to measure parameters of liquids, such as volume viscosity, surface tension, absorption, etc. The proposed ultrasonic approach to excitation of liquid/liquid interface appears to be especially promising in the experiments on liquid dynamics carried out at microgravity. These conditions are known to be implemented on the board of an orbital station or on the board of special aircrafts flying along a parabolic trajectory. In all these cases, strict requirements are imposed on the sizes and weight of experimental equipment. In this context, the ultrasonic method and equipment have evident advantages over their nonacoustic analogs, which are generally cumbersome and heavy.

The practical interest in the second mode of ultrasonic impact on liquid/liquid interface can be related to the development of all modern technologies requiring precise and (when necessary, remote) dosing of liquids in small volumes. Examples are synthesis of new materials, as well as biomedical, chemical, pharmacological, perfumery, food, and other technologies.

Finally, the third mode can be applied in preparation of emulsions and suspensions and in other processes implying intense stirring of different components.

ACKNOWLEDGEMENTS

This work was supported in part (within the project "Patterns and Surfaces") by the Marie Curie International Research Staff Exchange Scheme (IRSES) Fellowship of the 7th European Community Framework Program (No. 269207), the French Space Agency CNES, the ESA Topical Team "Liquid Interfaces Subjected to Oscillations", RFBR Project 14-02-93105, and the Grant NSh-4484.2014.2 of the Council of the President of the Russian Federation for Support of Young Scientists and Leading Scientific Schools.

REFERENCES

1. R.W. Wood and A.L. Loomis, "The Physical Effects of High-Frequency Sound Waves of Great Intensity," *Philos. Mag.* **7**, 417 (1927).
2. R.J. Lang, "Ultrasonic Atomization of Liquids," *J. Acoust. Soc.* **34**(1), 6 (1962).
3. R.G.M. Boucher and J. Kreuter, "Fundamentals of the Ultrasonic Atomization of Medicated Solutions," *Ann. Allergy.* **26**, 59 (1968).
4. K.A. Krause, "Focusing Ink Jet Head," *IBM Tech. Disclosure Bull.* **16**(4), 1168 (1973).
5. R.N. Ellson, "Picoliter: Enabling Precise Transfer of Nanoliter and Picoliter Volumes," *Drug Discovery Today.* **7**(5) (Suppl.), S32 (2002).
6. Yin Nee Cheung, Nam Trung Nguyen, and Teck Neng Wong, "Droplet Manipulation in a Microfluidic Chamber with Acoustic Radiation Pressure and Acoustic Streaming," *Soft Matter.* **10**, 8122 (2014).
7. A. Miglani and S. Basu, "Sphere to Ring Morphological Transformation in Drying Nanofluid Droplets in a Contact-Free Environment," *Soft Matter.* **11**, 2268 (2015).
8. B. Issenmann, A. Nicolas, R. Wunenburger, S. Manneville, and J.-P. Delville, "Deformation of Acoustically Transparent Fluid Interfaces by the Acoustic Radiation Pressure," *Europhys. Lett.* **83**(3), 34002 (2008).
9. B. Issenmann, A. Nicolas, R. Wunenburger, S. Manneville, and J.-P. Delville, "Experimental Confirmation of the Theory of Acoustic Radiation Pressure Applying on Transparent Interfaces," *J. Acoust. Soc. Amer.* **65**(6), 123 (2008).
10. R. Wunenburger, A. Casner, and J.-P. Delville, "Light-Induced Deformation and Instability of a Liquid Interface. I. Statics," *Phys. Rev. E.* **73**(3), 036314 (2006).
11. A. Casner, J.-P. Delville, and I. Brevik, "Asymmetric Optical Radiation Pressure Effects on Liquid Interfaces under Intense Illumination," *J. Opt. Soc. Amer. B.* **20**(11), 2355 (2003).